ChemPubSoc Europe

DOI: 10.1002/slct.201600119

Chemistry SELECT Communications

Electro, Physical & Theoretical Chemistry

In-Situ Spectro–electrochemical Insight Revealing Distinctive Silicon Anode Solid Electrolyte Interphase Formation in a Lithium–ion Battery

Junfeng Yang,[a, b] Nickolay Solomatin,[a] Alexander Kraytsberg,[a] and Yair Ein-Eli*[a, c]

The formation and evolution of solid electrolyte interphase (SEI) layer on a silicon electrode in 1 M $LiPF_6$ in EC/DMC electrolyte is investigated by in-situ FTIR spectroscopy. The results point that lithium alkyl carbonates formation is initiated during a lithiation process via a one-electron reduction of EC/DMC, followed by a free radical reaction. Interesting enough, the studies indicate that most of the SEI material is actually formed in the delithiation process. Carbon dioxide (CO_2) generated at low potentials during the shallow lithiation process is consumed during a deeper lithiation process and also during subsequent delithiation processes, resulting in the formation of lithium carbonate.

It has been well established that a stable solid electrolyte interphase (SEI) film plays a crucially role in lithium ion battery anode cyclability, coulombic efficiency and safety.[1] Unfortunately, the SEI layer is unstable on the silicon anode material and thickens upon cycling, leading to a rather poor performance and limiting silicon as a viable anode.[2,3] Extensive studies on the topic were conducted using *ex-situ* techniques (SEM, FTIR, XPS).[4] However, *ex-situ* methods unavoidably cause artifacts.[4d–4f] In contrast, *in-situ* techniques can provide convincing and detailed information on the SEI film formation and evolution.[5] Generally, *in-situ* FTIR is proven to be an efficient method to investigate SEI layer formation.[6] However, in situ FTIR studies of the SEI films on Si-powdered electrode have been rarely reported;[7] the strong IR absorption by the electrolyte, carbon black, and the Si powder are apparent barriers for such studies.[8] In this work, an accurate analysis of the SEI formation and evolution on the silicon powder electrode is being reported. For that purpose, *in-situ* ATR-FTIR spectro-electrochemical cell was developed, enabling eventually, a modification of a conventional wisdom on how the SEI is being formed on the brittle silicon anode in Li-ion batteries.

Details on silicon powder material's morphology, composition and crystallinity are provided in the Supporting Information, **Figure S1.** Potential *vs.* specific capacity plot for the first polarization cycle of the Si electrode is shown in Figure 1**a**. Lithium-Si alloying curve comprises of a rapid potential drop (from OCP to 1.3 V) followed by a steep slope (from 1.2 to 0.11 V) and a plateau (between 0.11 and 0.01 V). The lithiation onset potential is around 0.11 V, in a good agreement with the onset lithiation potential for silicon nanowire anodes.[3] Differential capacity plot (Figure 1**b**) reveals a tiny peak at ~ 0.87 V and a pronounced peak at ~50mV in the lithiation branch. The peak at ~ 0.87 V can be attributed to the formation of SEI on the Si anode. Such peak, which precedes the lithiation, is commonly attributed to the SEI formation, and its particular potential strongly depends on the specific silicon material structure.[3,9] The sharp peak during lithiation, appearing at ~50mV, originates from a phase transformation from amorphous Li_xSi to crystalline $Li_{3.75}Si$, whereas the two pronounced anodic peaks in the delithiation process, (at 0.32 and 0.48 V)are ascribed to a phase transition in the Li_xSi alloy.[10]

Until now, three types of *in-situ* FTIR–ATR cell configurations were designed and employed to enable monitoring the electrode's surface chemistry. Detailed description of theirs designs and associated challenges are shown and discussed in **Scheme S1 a–c**, Supporting Information. We designed *in-situ* FTIR-ATR spectro-electrochemical half-cell (**Scheme S1 d**), overcoming these challenges.

I*n-situ* FTIR spectra were acquired from Si electrodes polarized to a desired potential; the potentials and corresponding FTIR spectra are shown in **Figures 1 a** and **2 a**, respectively. The FTIR spectra obtained from the pristine Si electrode (before assembling) are very weak, and do not reveal observable absorption bands. Subsequent to the cell assembling and a 12 hours stay in a glove box, the Si electrode was cathodically polarized at C/100 rate, allowing an accurate spectroscopic analysis at each pre-determined potential. FTIR spectrum acquired at 0.8 V (spectrum II) presents several IR bands, all assigned to the electrolyte. The electrolyte's FTIR spectrum and the specific IR bands assignments are presented in **Figure S2** and **Table S1.** Spectra III–VI obtained from the electrode, which was progressively lithiated to 0.1 V, are all quite similar to spectrum II (0.8 V).The absence of the SEI-based absorbance bands in the

[a] *Dr. J. Yang, N. Solomatin, Dr. A. Kraytsberg, Prof. Y. Ein-Eli*
Department of Materials Science and Engineering
Technion-Israel Institute of Technology, Haifa, 3200003 (Israel)
[b] *Dr. J. Yang*
Institute of Solid State Physics
Key Laboratory of Materials Physics
Chinese Academy of Sciences, Hefei 230031, China
[c] *Prof. Y. Ein-Eli*
The Nancy & Stephen Grand Technion Energy Program, Technion-Israel Institute of Technology, Haifa, 3200003 (Israel)
Fax: (+972)-4-829-5677
E-mail: eineli@tx.technion.ac.il

Supporting information for this article is available on the WWW under http://dx.doi.org/10.1002/slct.201600119

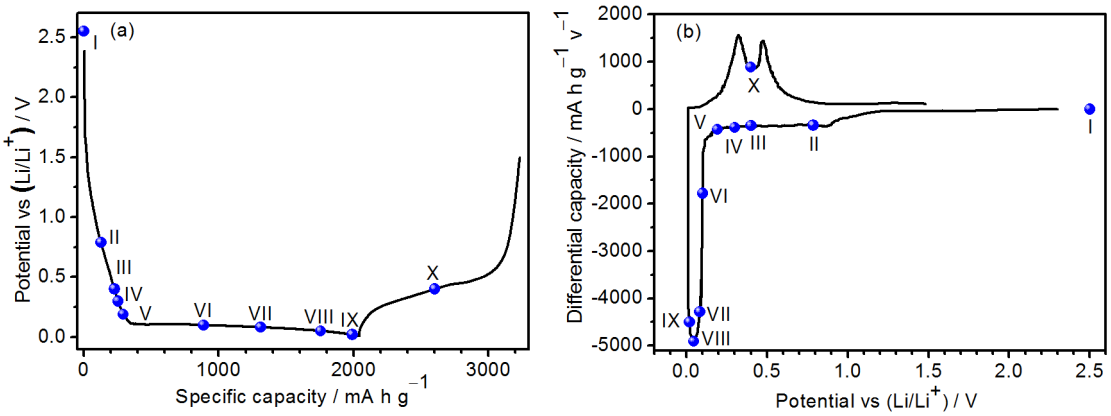

Figure 1. (a) Voltage *vs.* specific capacity and **(b)** a the corresponding differential capacity (dQ/dV) *vs.* voltage for a silicon electrode in the first cycle (at C/100). Polarization *vs.* Li metal was conducted starting from OCP to 0.01 V during lithiation, and starting from 0.01 to 1.5 V during delithiation. Dots indicate the specific potentials at which the FTIR spectra were acquired.

spectra needs an explanation, as the differential capacity plot (Figure 1**b**) clearly indicates that the SEI formation starts at ~0.87 V. For this end, the electrode was cycled between 1.5 V and 0.8 V and the observable surface specie's absorbance bands appear only after 30 cycles, and then they steadily grow up upon cycling (**Figure S3**).

It is a good ground to suggest that in the potential window of 0.8-0.1 V (corresponding to spectra (II) – (VII)) the SEI-film indeed do exist, albeit it is too thin to maintain a distinct IR-absorption band. This observation is in a good consistency with the current conceptions of Si anode SEI-film development upon cycling. Currently, it is assumed that the SEI-film does not fully adhere to the Si-particle surface during cycling but peels off to a certain extent because of large Si volume changes.[11, 12]Upon further and deeper lithiation process, observation of SEI affiliated IR absorption commences. Several new IR bands appear at a potential of 80mV [~1642 ($\upsilon_{asC=O}$), ~1394 (υ_{sC-H}) and ~1342 cm^{-1} ($\upsilon_{sC=O}$), along with the increase in the intensity of the IR bands at ~1286 ($\upsilon_{sC=O}$), ~1069 (υ_{sC-O}) and ~835 cm^{-1} (δ_{OCO2})]. These bands may be assigned to mixture of lithium alkyl carbonates CH_3OCO_2Li, $(CH_2OCO_2Li)_2$, and $CH_3CH_2OCO_2Li$.[13] Considering the obvious broadening of the C=O band, one may suggest the formation of these species *via* a single electron reduction, followed by a radical termination reaction, as shown in **Reaction Scheme RS1 a.**[1b, 1c, 13] No new IR band emerges, as the electrode is further polarized to 50 mV and then down to 10 mV; the intensity of the IR bands, corresponded to lithium alkyl carbonates, gradually increased during polarization. This suggests a continuous formation of a film during the deep Si lithiation process.

Differential absorbance spectra (absorbance obtained at a specific potential minus the absorption at 0.8 V) obtained from the Si-electrode are presented in Figure 2**b**. In this representation, the upward absorbance bands indicate an increase in the accumulative amount of the corresponding species relative to 0.8 V, and vice versa. The IR absorbance pattern is the same for 0.8, 0.4, 0.3 and 0.2 V, but some new bands gradually appear starting from 0.11 V. The emerged upward bands may be attributed either to new evolving surface species or to free solvent molecules. Such solvent molecules are formed because lithium ions are leaving their solvation spheres as these ions participate in the alloying process. Conversely, the downward absorption bands may be related to the IR-absorption of the solvent molecules incorporated into solvation spheres of the Li ions - $Li(solvent)^+$. Expectably, the concentration of $Li(solvent)^+$ diminishes with the development of the lithiation process. An IR band couple (upward absorption band at 1802 $cm^{-1}$and downward band at 1782 cm^{-1}) is attributed to C=O group of non-solvated and solvated EC molecules, respectively (C=O vibration is weakened by solvation[14]). The υ_{C-O-C} and υ_{C-O} bands of non-solvated DMC and non-solvated EC at 1306, 1157 and 1071 cm^{-1} are the upward bands, whereas the corresponding bands of the solvated DMC and EC species are the downward bands at 1317, 1199 and 1087 cm^{-1}(the C–O and C–O–C bonds are strengthened by the solvation[15]). Several pairs of bands (at 1247/1273, 891/913, 782/793 and 714/724 cm^{-1}) correspond to non-solvated/solvated O–C–O(DMC), CH_3-O(DMC), O-CO_2(DMC) and EC - ring; evolvement of these bands indicates that the solvation can strengthen these bonds. Other upward bands are assigned to the newly formed SEI film, appearing due to electrolyte decomposition.

The intensity of the IR-absorption bands increases substantially during Li^+ extraction (0.36 V) from the Li_xSi alloy. The IR bands at 723, 900 and 980 cm^{-1} are attributed to the formation of alkyl phosphates, as a result of $LiPF_6$ decomposition and further reactions of these decomposition products with ROH and ROLi species.[16] The intensity of the 1765 cm^{-1} band substantially increases; the EC-associated C=O group has the absorption band with the same wavelength, but the substantial difference between the intensities of the 1802 and 1765 cm^{-1} bands and the appearance of a new and strong band at 1196 cm^{-1}(with a shoulder at 1157 cm^{-1}) suggests the formation of surface polycarbonates, possibly originate from EC and DMC polymerization[17], while the peak at ~1320 cm^{-1} may

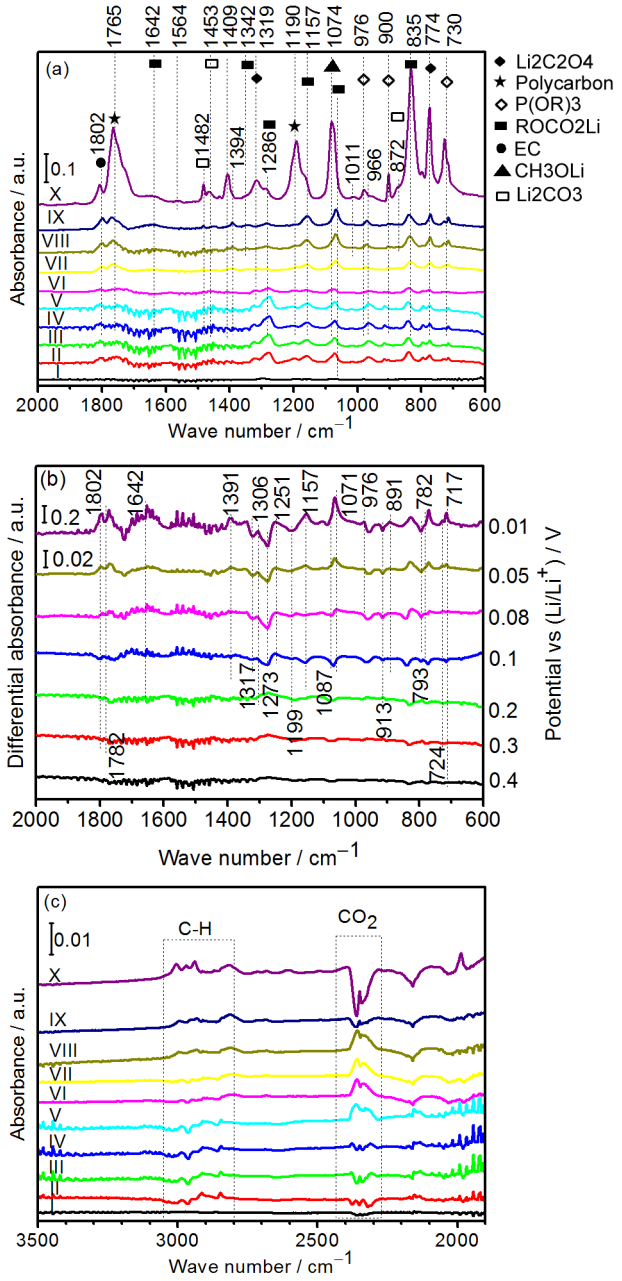

Figure 2. (a) Differential FTIR spectra relative to the spectra obtained at 0.8 V during lithiation/delithiation; **(b)** *In-situ* FTIR spectra of silicon powder electrode upon lithiation to different potentials: (I) represents the as-prepared working electrode, II–IX represent the lithiation potentials of 0.8, 0.4, 0.3, 0.2, 0.1, 0.08, 0.05, 0.01 V, respectively. X represents potential of 0.4 V during delithiation; **(c)** *In-situ* FTIR spectra in the wave number region of 1900–3500 cm^{-1}: I–X spectra present the same potential as in (b).

be attributed to the formation of Li-oxalate.[18] This suggests the ample formation of SEI-related material accumulating onto the electrode during delithiation-type polarization.

The SEI film is formed initially on the pristine silicon particle surface during the cathodic polarization, and only then a formation of an additional SEI film material occurs on newly exposed Li_xSi surfaces. These sites are being exposed since the initially formed SEI film cracks. Indeed, the cracks appear in course of lithiation upon Si-particle expansion exposing fresh Li_xSi surface, as it is illustrated in Scheme 1**a**. It is in consistency with the results on the resistance of SEI (R_{SEI}) on Si-electrode.[19,20] Overall, the SEI-material amount is determined by the surface area of the fully expanded Li_xSi. Upon delithiation, Li_xSi core, which supports the SEI-film shell, actually shrinks and the SEI shell crumbles (Scheme 1**b**) and thus large area of shrinking Li_xSi core is turning to be bare and exposed to the electrolyte, and thus is available for a fresh SEI-layer build-up. This situation repeats several times during Li-ion extraction, leading to a substantial accumulation of SEI-film material during delithiation.

The reports on the SEI's morphology developed on flat Si-film electrode in different electrolytes supports this presumption.[21,22] Recent theoretical study suggests the appearance of large non-uniform stresses inside the SEI-film during its growth and lithiation/delithiation process.[23] It was shown that SEI layers formed on the lithiated (expanded) Si, experience high compressive stresses upon delithiation. The stresses are related to the large normal tensile tractions across the anode/SEI-film interface, resulting in SEI-delamination. It was demonstrated that the shape of the electrode particles does matter; specifically, spheroidal particle shape results in appearance of substantially higher (~3 times higher) normal traction forces at the particle/SEI interface than spherical particles.[23] Unfortunately, up to now, there are no experimental investigations of SEI-film mechanics onto an individual Si-particle.

Importantly, no evidence of lithium carbonate (Li_2CO_3) formation during lithiation process was found. However, a high frequency shoulder (of the 835 cm^{-1} band) appears at 872 cm^{-1} during delithiation process. The appearance of this sholder, along with the increase in the 1482 and 1453 cm^{-1} bands intensities, suggests the formation of Li_2CO_3 during the delithiation process. Previous studies demonstrated that Li_2CO_3 could be formed by a direct two-electron reduction of EC.[24] The absence of Li_2CO_3 along with lithium alkyl carbonates formation may suggest that EC and DMC reduction follows a single electron pathway upon lithiation, whereas a double electron pathway is suppressed at low current densities.

The spectra in the 2850–3002 cm^{-1} region (Figure 2**c**) is attributed to the stretching modes of CH_3- and -CH_2- demonstrating the presence of alkyl group;[25] the evolution of the 2300–2400 cm^{-1} bands corresponded to CO_2 formation is observed. Carbon dioxide IR bands are negative at potentials above 0.3 V, since CO_2 concentration in the electrochemical cell is smaller than the concentration in the background atmosphere; carbon dioxide bands are upward as the potential decreases from 0.3 to 0.2 V indicating the formation of a large amount of this substance. Carbon dioxide could be generated *via* a reaction of lithium alkyl carbonate either with HF (HF is unavoidable contaminant of $LiPF_6$ salt) or with water in the electrolyte; the latter is unlikely, though, because of the absence of Li_2CO_3 absorbance bands. According to **Reaction Scheme RS1 b**[1c,4f,13d] LiF can be formed, albeit LiF is IR inactive.[4d,26] CO_2-band begins to adopt the downward character because of CO_2-reduction as the electrode is polarized down to 10mV. Consumption of CO_2 continues during delithiation up to

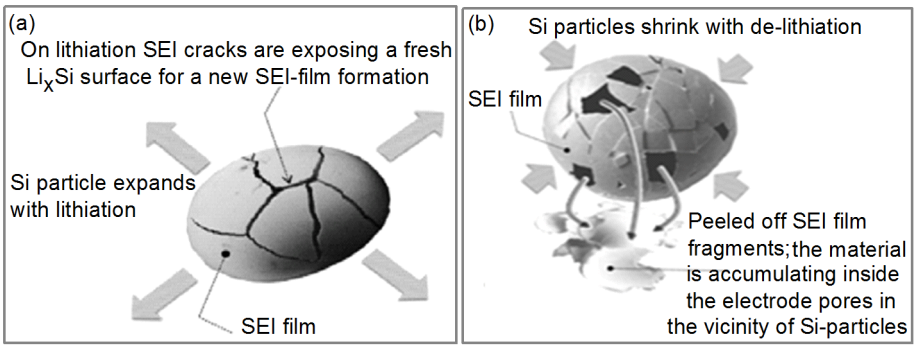

Scheme 1. Schematic presentation of the SEI-film formation, destruction and rearrangements in the course of silicon **(a)** lithiation and **(b)** delithiation processes.

0.36 V, and this character is intensified as CO_2 further reacts. The appearance of Li_2CO_3 during delithiation process is summarized in **Reaction Scheme RS1 c.**[1b,4e]

In summary, the reactions, which are involved in the SEI formation, gas evolution and lithium ions solvation/de-solvation were *in-situ* revealed, *via* a thorough monitoring of the processes at the Si electrode/electrolyte interface. The conclusions derived from this eye-opening research are: **(1).** Electrolyte decomposition follows a one-electron reduction pathway during lithiation at a low current density, leading to the formation of lithium alkyl carbonates, whereas electrolyte salt decomposition takes place over a fresh Li_xSi surface, forming alkyl phosphates at potentials below 0.4 V; **(2).** CO_2 is formed *via* a chemical reaction of lithium alkyl carbonate with HF; it reacts with free radicals or lithium ions, producingLi_2CO_3during subsequent delithiation process; **(3).** Silicon particle contraction results in SEI-shell peeling-off, and thus Li_xSi particle surface may be freshly exposed to the electrolyte several times during delithiation process; **(4).** Most of the electrolyte decomposition products are rather formed during delithiation process. These "take-home" messages are quite unique, as they have a substantial impact on a proper silicon anode design for Li-ion batteries, as it extends the basic understanding of the SEI nature, its build-up and disruption mechanisms.

Acknowledgements

The authors acknowledge the support from the EU FP7 Grant Award No. 608491-Battery and Supercapacitors Characterization and Testing (BACCARA) Project, Israel Science Foundation (ISF) Grant Award No. 2792/11-Israel National Research Center for Electrochemical Propulsion (INREP) and the Grand Technion Energy Program (GTEP).

Keywords: solid-electrolyte interphase · silicon · Li- ion battery · FTIR spectroscopy · Interface

[1] a) E. Peled, *J. Electrochem. Soc.* **1979**, *126*, 2047; b) D. Aurbach, B. Markovsky, I. Weissman, E. Levi, Y. Ein-Eli, *Electrochim. Acta* **1999**, *45*, 67; c) D. Aurbach, B. Markovsky, A. Shechter, Y. Ein-Eli, H. Cohen, *J. Electrochem. Soc.* **1996**,*143*, 3809.

[2] a) M. N. Obrovac, L. J. Krause, *J. Electrochem. Soc.* **2007**, *154*, A103; b) B. Liang, Y. Liu, Y. Xu, *J. Power Sources* **2014**, *267*, 469.

[3] C. K. Chan, R. Ruffo, S. S. Hong, Y. Cui, *J. Power Sources* **2009**, *189*, 1132.

[4] a) B. T. Young, D. R. Heskett, C. C. Nguyen, M. Nie, J. C. Woicik, B. L. Lucht, *ACS Appl. Mater. Interfaces* **2015**, *7*, 20004; b) G. M. Veith, M. Doucet, J. K. Baldwin, R. L. Sacci, T. M. Fears, Y. Wang, J. F. Browning, *J. Phys. Chem. C.* **2015**, *119*, 20339; c) F. Luo, G. Chu, X. Xia, B. Liu, J. Zheng, J. Li, H. Li, C. Gu, L. Chen, *Nanoscale* **2015**, *7*, 7651; d) K. Edström, M. Herstedt, D. P. Abraham, *J. Power Sources* **2006**, *153*, 380; e) D. Aurbach, Y. Gofer, M. Ben-Zion, P. Aped, *J. Electroanal. Chem.* **1992**, *339*, 451; f) D. Aurbach, M. L. Daroux, P. W. Faguy, E. Yeager , *J. Electrochem. Soc.* **1987**, *134*, 1611.

[5] P. P. R. M. L. Harks, F. M. Mulder, P. H. L. Notten, *J. Power Sources* **2015**, *288*, 92.

[6] a) Y. Ikezawa, H. Nishi, *Electrochim. Acta* **2008**, *53*, 3663; b) C. M. Burba, R. Frech, *Electrochim. Acta* **2006**, *52*, 780.

[7] D. Alves Dalla Corte, G. Caillon, C. Jordy, J. N. Chazalviel, M. Rosso, F. Ozanam, *Adv. Energy Mater.* **2016**, *2*,1501768

[8] J. T. Li, S. R. Chen, F. S. Ke, G. Z. Wei, L. Huang, S. G. Sun, *J. Electroanal. Chem.* **2010**, *649*, 171.

[9] J. Graetz, C. C. Ahn, R. Yazami, B. Fultz, *Electrochem. Solid-State Lett.* **2003**, *6*, A194.

[10] B.A. Boukamp, G.C. Lesh, R.A. Huggins, *J. Electrochem. Soc.* **1981**, *128*, 725.

[11] E. Radvanyi, W. Porcher, E. De Vito, A. Montani, S. Franger, S. Jouanneau Si Larbi, *Phys. Chem. Chem. Phys.* **2014**, *16*, 17142.

[12] M. Y. Nie, D. P. Abraham, Y. J. Chen, A. Bose, B.L. Lucht, *J. Phys. Chem. C.* **2013**, *117*, 13403.

[13] a) J. S. Kim, Y. T. Park, *J. Power Sources* **2000**, *91*, 172; b) Y. S. Hu, W. H. Kong, H. Li, X. J. Huang, L. Chen, *Electrochem. Commun.* **2004**, *6*, 126; c) J. S. Shin, C. H. Han, U. H. Jung, S. I. Lee, H. Jin, Kim, K. Kim, *J. Power Sources* **2002**, *109*, 47; d) D. Aurbach, Y. Ein-Eli, O. Chusid, Y. Carmeli, M. Babai, H. Yamin, *J. Electrochem. Soc.* **1994**, *141*, 603; e) D. Aurbach, A. Zaban, *J. Electrochem. Soc.* **1995**, *142*, L108.

[14] M. Masia, M. Probst, R. Rey, *J. Phys. Chem. B.* **2004**, *108*, 2016.

[15] J. T. Li, S. R. Chen, X. Y. Fan, L. Huang, S. G. Sun, *Langmuir* **2007**, *23*, 13174.

[16] U.S. Vogl, S. F. Lux, E. J. Crumlin, Z. Liu, L. Terborg, M. Winter, R. Kostecki, *J. Electrochem. Soc.* **2015**, *162*, A603.

[17] R. Yazami, *Electrochim. Acta* **1998**, *45*, 817.

[18] S. Dalavi, P. Guduru, B.L. Lucht, *J. Electrochem. Soc.* **2012**, *159*, A642.

[19] E. Radvanyi, K. Van Havenbergh, W. Porcher, S. Jouanneau, J. S. Bridel, S. Put, S. Franger, *Electrochim. Acta* **2014**, *137*, 751.

[20] B. Jerliu, E. Hüger, L. Dörrer, B.K. Seidlhofer, R. Steitz, V. Oberst, U. Geckle, M. Bruns, H. Schmidt, *J. Phys. Chem. C.* **2014**, *118*, 9395.

[21] L.B. Chen, K. Wang, X. H. Xie, J. X. Xie, *J. Power Sources* **2007**, *174*, 538.

[22] V. Kuznetsov, A.H. Zinn, G. Zampardi, S. Borhani-Haghighi, F. La Mantia, A. Ludwig, W. Schuhmann, E. Ventosa, *ACS Appl. Mater. Interfaces* **2015**, *7*, 23554.
[23] E. Rejovitzky, C.V. Di Leo, L. Anand, *J. Mech. Phys. Solids* **2015**, *78*, 210.
[24] a) C.C. Nguyen, B.L. Lucht, *J. Electrochem. Soc.* **2014**, *161*, A1933; b) Q. L. Zhang, X. C. Xiao, W. D. Zhou, Y. T. Cheng, M.W. Verbrugge, *Adv. Energy Mater.* **2015**, *5*, 1401398
[25] G.V. Zhuang, H. Yang, B. Blizanac, P.N. Ross, *Electrochem. Solid-State Lett.* **2005**, *8*, A441.
[26] D. Aurbach, B. Markovsky, A. Rodkin, M. Cojocaru, E. Levi, H.J. Kim, *Electrochim. Acta.* **2002**, *47*, 1899.
[27] J. Yang, A. Kraytsberg and Y. Ein-Eli, *J. Power Sources* **2015**, *282,* 294

Submitted: February 16, 2016
Accepted: March 9, 2016